ELSEVIER

Journal of Organometallic Chemistry 650 (2002) 43–56

Journal of Organometallic Chemistry

www.elsevier.com/locate/jorganchem

# The marked influence of steric and electronic properties of ancillary pyridylthioether ligands on the rate of allene insertion into the palladium–carbon bond

Luciano Canovese [a,*], Fabiano Visentin [a], Gavino Chessa [a], Claudio Santo [a], Paolo Uguagliati [a], Giuliano Bandoli [b]

[a] *Dipartimento di Chimica, Calle Larga Santa Marta, Università degli Studi di Venezia, 2137-30123 Venice, Italy*
[b] *Dipartimento di Scienze Farmaceutiche, Università di Padova, Padua, Italy*

Received 7 September 2001; accepted 7 January 2002

**Abstract**

Neutral methyl- and acyl-palladium chloro complexes containing pyridylthioether ancillary ligands (R′N–SR) (R′ = H, Me, Cl; R = Me, Et, *i*-Pr, *t*-Bu, Ph) have been synthesised and characterised by elemental analysis and spectroscopic methods. The reactivity of these complexes toward allene (allene = DMA = 1,1-dimethylpropadiene; TMA = 1,1,3,3-tetramethylpropadiene) insertion into the palladium–carbon bond has been studied by $^1$H-NMR and UV–vis techniques. The rate of reaction appears to be strongly influenced by the steric and electronic properties of the ancillary ligand. The distortion induced by the substituent R′ in position 6 of the pyridine ring on the main coordination plane of the substrate (allowed by sulphur $sp^3$ hybridisation) renders the substrate itself more prone to nucleophilic attack by the allene. The rate of allene insertion can further be enhanced by lowering the basicity of the chelating atoms in the N–S moiety which results in an increase of electrophilicity of the palladium core, so that the rate constants measured in the case of the complexes containing the ligand 6-chloro-2-phenylthiomethylpyridine (ClN–SPh) are by far the greatest observed so far for similar reactions. Furthermore, on the basis of the indications emerging from the exhaustive study on the behaviour of all the related pyridylthioether methyl complexes, an associative asynchronous bond making mechanism for the rate determining nucleophilic attack by allene is proposed. © 2002 Elsevier Science B.V. All rights reserved.

*Keywords:* Allene; Pyridylthioether; Palladium–carbon bond; Insertion mechanism

## 1. Introduction

We are currently studying the mechanism of allene insertion into the palladium–carbon bond in pyridylthioether methyl complexes of type [PdCl(Me)(R′N–SR)] (R′N–SR = 6-R′-$C_5H_3N$-2-$CH_2SR$) to give [Pd($\eta^3$-2-methylallyl)(R′N–SR)]$^+$ [1].

The interaction of organopalladium compounds with allenes is particularly important since, under catalytic conditions, assembly of allenes, carbon monoxide, and nucleophiles leads to allylamines, methacrylates, or heterocycles [2]. This is a particular issue of the more general field of the insertion of unsaturated molecules into the metal–alkyl and metal–aryl bonds in chelate complexes and its catalytic implications [3]. These reactions appear to be affected by the steric, electronic, and structural properties of the chelating ligand, although a variety of features may emerge, depending on the bite angle and rigidity of such ligand and its hemilability [4].

We have observed a remarkable rate enhancement of allene insertion induced by distortion of the coordination environment caused by the presence of a substituent in position six of the pyridine ring of the bidentate ligand R′N–SR [1]. As a matter of fact, such distortion will render the requisite preliminary step of these insertion reactions, i.e. prior coordination of the allene, much easier [3f, 4e,f]. Our work also hinted that the highest rate of allene insertion can be achieved by a combination of main coordination plane distortion and lowered basicity of coordinating atoms (N and/or S) in

* Corresponding author. Tel.: +39-41-5298567/68; fax: +39-41-5298517.
*E-mail address:* cano@unive.it (L. Canovese).

0022-328X/02/$ - see front matter 
PII: S0022-328X(02)01145-2

the chelating ligand. In fact, when the electron-withdrawing phenyl group is bound to sulphur, the highest second-order rate constant for allene insertion is obtained [1]. Thus, in our search for the most efficient factors enhancing the rate of allene insertion in these systems, we have conceived the idea of decreasing the basicity of both the pyridine nitrogen and of the sulphur in our pyridylthioether ligands while maintaining the distortion of the coordination plane and providing for sufficient stability of the metal–polydentate ring, as ensured by the high flexibility of the S-donor chelate ligand. To this aim, we have synthesised the ligands and the complexes in Scheme 1, where the methyl group bound to palladium is *trans* to the pyridine nitrogen (see further). We have also carried out a kinetic investigation of the reaction in order to confirm our hypothesis and to provide a comprehensive overview of the factors governing the mechanism of allene insertion.

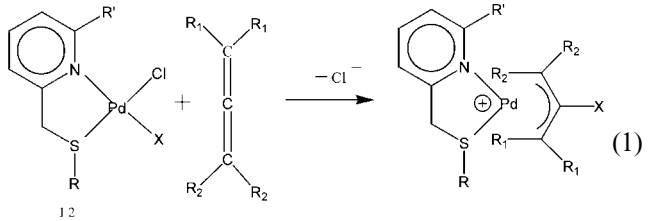


(1)

DMA : $R_1$ = H, $R_2$ = Me; TMA : $R_1$ = $R_2$ = Me ; X = Me, COMe

## 2. Results and discussion

### 2.1. Synthesis, characterisation and X-ray structure

Addition, under inert atmosphere ($N_2$), of the appropriate ligand (R′N–SR) to a toluene solution of [PdCl(Me)(COD)] yields the corresponding complexes [PdCl(Me)(R′N–SR)]. Reaction of a $CHCl_3$ solution of these complexes with carbon monoxide yields almost instantaneously the related acyl species [PdCl(COMe)(R′N–SR)]. The methyl and the acyl complexes react in $CH_2Cl_2$ with allenes DMA or TMA to give the allyl derivatives as reported in Scheme 1. All the new unpublished complexes were characterised by elemental analysis, IR spectroscopy and NMR spectrometry (see Section 3). In order to assess the relative positions of the palladium-bound methyl group and the pyridine nitrogen, we have carried out an X-ray structure determination of the complex [PdCl(Me)-(HN–SMe)]. The structure motif of the complex is given by the juxtaposition in the unit cell of two monomeric units (Fig. 1), which are virtually identical, the r.m.s. deviation of their superimposition being 0.05 Å, with the largest deviation (0.10 Å) shown by the C(8) methyl atom. The coordination around palladium is square-planar with the chloride and the sulphur of the pyridylthioether ligand *trans* to one another, the *cis*

**LIGANDS** :

R'N-SR

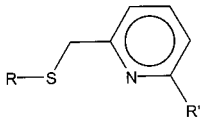


R' = H; R = Me, Et, *i*-Pr, *t*-Bu, Ph;

R' = Me; R = *t*-Bu, Ph;

R' = Cl; R = Me, *t*-Bu, Ph;

**COMPLEXES**:

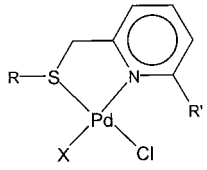


X = Me;

R' = H; R = Me, Et, *i*-Pr, *t*-Bu, Ph;

R' = Me; R = *t*-Bu, Ph;

R' = Cl; R = Me, *t*-Bu, Ph;

X =COMe;

R' = H; R = Me, Et, *i*-Pr, *t*-Bu, Ph

R' = Me; R = *t*-Bu, Ph;

R' = Cl; R = *t*-Bu;

**INSERTION PRODUCTS** :

$[Pd(\eta^3\text{–}(R_1)_2CC(R_3)C(R_2)_2)(R'N\text{-}SR)]^+$

R' = H; R = Me, Et, *i*-Pr, *t*-Bu, Ph; $R_1$ = $R_3$ = Me, $R_2$ = H;

R' = Me; R = *t*-Bu, Ph; $R_1$ = $R_3$ = Me, $R_2$ = H;

R' = Cl; R = Me, *t*-Bu, Ph; $R_1$ = $R_3$ = Me, $R_2$ = H;

R' = Me; R = *t*-Bu, Ph; $R_1$ = $R_2$ = $R_3$ = Me;

R' = Cl; R = Me, *t*-Bu, Ph; $R_1$ = $R_2$ = $R_3$ = Me;

R' = H; R = *t*-Bu; $R_1$ = Me, $R_2$ = H, $R_3$ = COMe;

R' = Me; R = *t*-Bu; $R_1$ = Me, $R_2$ = H, $R_3$ = COMe;

R' = Cl; R = *t*-Bu; $R_1$ = Me, $R_2$ = H, $R_3$ = COMe

Scheme 1.

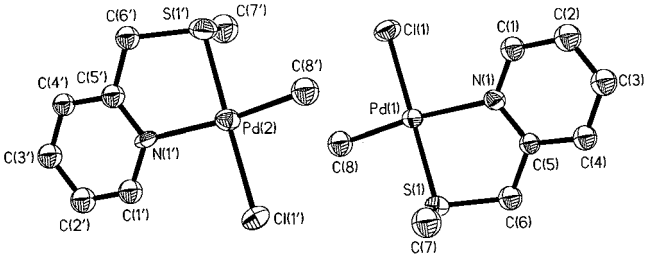


Fig. 1. ORTEP drawing of the asymmetric unit showing the atom numbering scheme and 50% displacement ellipsoids. Hydrogen atoms have been omitted for clarity.

Table 1
Selected bond lengths (Å) and bond angles (°)

| | | | |
|---|---|---|---|
| *Bond lengths* | | | |
| Pd(1)–S(1) | 2.257(5) | Pd(2)–S(1′) | 2.255(6) |
| Pd(1)–Cl(1) | 2.315(6) | Pd(2)–Cl(1′) | 2.340(6) |
| Pd(1)–N(1) | 2.16(1) | Pd(2)–N(1′) | 2.17(1) |
| Pd(1)–C(8) | 2.01(1) | Pd(2)–C(8′) | 2.00(1) |
| S(1)–C(6) | 1.81(1) | S(1′)–C(6′) | 1.79(1) |
| S(1)–C(7) | 1.79(2) | S(1′)–C(7′) | 1.81(2) |
| *Bond angles* | | | |
| S(1)–Pd(1)–N(1) | 84.1(4) | S(1′)–Pd(2)–N(1′) | 83.8(4) |
| S(1)–Pd(1)–C(8) | 88.8(6) | S(1′)–Pd(2)–C(8′) | 89.6(6) |
| Cl(1)–Pd(1)–N(1) | 95.3(4) | Cl(1′)–Pd(2)–N(1′) | 95.7(4) |
| Cl(1)–Pd(1)–C(8) | 91.6(6) | Cl(1′)–Pd(2)–C(8′) | 90.7(6) |
| S(1)–Pd(1)–Cl(1) | 177.6(2) | S(1′)–Pd(2)–Cl(1′) | 176.2(2) |
| N(1)–Pd(1)–C(8) | 172.3(7) | N(1′)–Pd(2)–C(8′) | 173.2(7) |
| Pd(1)–S(1)–C(6) | 99.3(6) | Pd(2)–S(1′)–C(6′) | 99.3(5) |
| Pd(1)–S(1)–C(7) | 104.4(7) | Pd(2)–S(1′)–C(7′) | 102.0(7) |
| C(6)–S(1)–C(7) | 100.6(9) | C(6′)–S(1′)–C(7′) | 99.9(8) |
| S(1)–C(6)–C(5) | 112(1) | S(1′)–C(6′)–C(5′) | 113(1) |

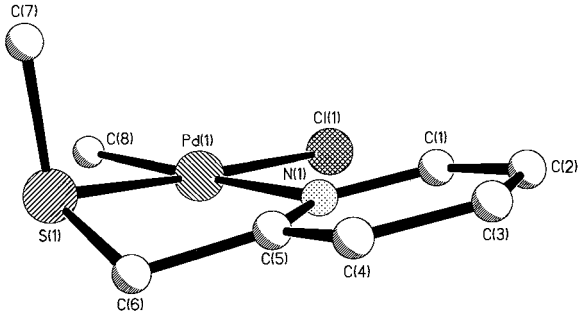


Fig. 2. A perspective view of the complex showing the C(6) atom below (by 0.50 Å) and the C(7) atom above (by 1.73 Å) the mean coordination plane.

bond angles ranging from 83.8 to 95.7° and the *trans* angles between 172.3 and 177.6° (Table 1). In both units the palladium atom is out of the mean coordination plane by 0.05 Å, the N···S bite distance is 2.96 Å and the N–Pd–S bite angle is equal within error [84.1 (4) and 83.8 (4)°], while the values for the dihedral angles between the mean coordination plane and the six-membered ring are slightly different [13.3(5) and 10.4(6)°] as well as the Pd–S(1)–C(7) angles [104.4(7) and 102.0(7)°].

In the five-membered ring the C(6) atom is out by 0.49 Å (0.47 Å in the other unit) from the Pd–N(1)–C(5)–S(1) mean plane (Fig. 2) and the two bond angles at sulphur, Pd–S(1)–C(6) and C(7)–S(1)–C(6), approach 100° [99.3(6)–100.6(9)° and 99.3(5)–99.9(8)°, respectively].

A comparison with the previously reported palladium(0) complex containing the same pyridylthioether bidentate ligand, i.e. [Pd($\eta^2$-tcne)(HN–SMe)] [5] shows that, on going from the oxidation number 0 to II, the Pd–S distance of 2.352(3) Å shortens to 2.256 Å and on the contrary, the Pd–N separation lengthens from 2.091(7) to 2.16 (1) Å, the S–Pd–N bite angle remaining virtually unchanged at ca. 83.5°.

Other metrical parameters compare favourably with the expected values, as can be seen by looking at the data retrieved in version 5.19 (April 2000) of Cambridge Structural Database (CSD) [6]. In particular the mean value for the Pd–Cl lengths observed in this complex (2.328(6) Å) parallels that of 2.335 Å encountered in other 1512 Pd–Cl entries whereas the Pd–C(8) separation of 2.01(1) Å is slightly shorter than the mean value (2.037 Å) observed in sixty Pd–$C_{methyl}$ determinations.

In the unit cell the minimum Pd···Pd separation is 3.769 Å and the only, somewhat, short interactions (in the range 2.71–2.78 Å) involve the chloride ligands with the phenyl hydrogens at C(4) and C(6).

### 2.2. Solution behaviour

#### 2.2.1. Methyl complexes

The NMR investigations on the methyl derivatives [PdCl(Me)(R′N–SR)] (R′ = H, Me) indicate the presence of one single isomer, in which the pyridylthioether ligand acts as a bidentate since only one Pd–C$H_3$ protons signal is observed, among other pieces of evidence. The complete characterisation of these complexes requires low temperature studies since all these species undergo fluxional rearrangement at room temperature. From theoretical considerations based on the mutual *trans* influence between the methyl group and the sulphur atom [4d,7] and the available structural determinations reported in this paper and elsewhere, [1] we conceive the hypothesis that the most likely isomer is the species in which the palladium coordinated methyl group lies *trans* to the pyridine nitrogen. The observed fluxional behaviour of these substrates can be easily traced back to the pyramidal sulphur inversion [8]; in fact on increasing temperature the observable AB quartet due to diastereotopic C$H_2$S protons disappears yielding a broad singlet. Apparently the chirogenic nature of sulphur is lost upon inversion of its absolute configuration and such a phenomenon appears to be independent of substrate concentration in conformity with the intramolecular sulphur rearrangement which is known to be of widespread occurrence in both Pd(0) and Pd(II) complexes [5,9]. Moreover, detailed investigations by dynamic NMR on some substrates support this conclusion since the calculated activation parameters are in agreement with this mechanistic picture [10].

The room temperature $^1$H-NMR spectra of the complexes [PdCl(Me)(ClN–SR)] display quite different features since the observed fluxional behaviour cannot be traced back only to sulphur inversion. As a matter of fact the room temperature spectrum of the complex [PdCl(Me)(ClN–S′Bu)] exhibits a collapsing AB system

($CH_2S$ protons) and an incipient broadening of the signals ascribable to *t*-Bu methyl groups ($\delta = 1.31$ ppm), to Pd–$CH_3$ protons ($\delta = 1.16$ ppm) and to the partially obscured pyridine $H^5$ ($\delta \cong 7.5$ ppm). These pieces of evidence suggest the presence of a fast sulphur inversion coupled with a process involving a fast rearrangement between isomers. As a matter of fact either decreasing or increasing the temperature lead to a spectrum simplification. The low temperature spectrum is in accord with a 'frozen' situation in which only the predominant N–Me *trans* isomer (hereafter *trans*) is observable. The high temperature spectrum suggests a very rapid interchange between the species as indicated in the following scheme. The resulting average spectrum takes into account the presence of the N–Me *cis* isomer (hereafter *cis*) in small concentration, as can be seen from the tell-tale chemical shift and shape of the pyridine $H^5$ which happens to be markedly affected by the *trans* influence of the group *trans* to pyridine.

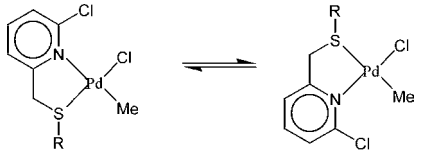


N-Me *trans* N-Me *cis*

Thus, at variance with the complexes bearing R′N–SR (R′ = H, Me) ligands the 6-chloro substituted pyridylthioeter complexes undergo fast interchange between *trans* and *cis* isomers probably owing to the low basicity of the pyridine nitrogen [14] and the high *trans* influence of the methyl group. However, thermodynamic parameters for the above *cis–trans* equilibrium could not be determined owing to the very large difference in population between isomers.

Other interpretations involving adventitious nucleophiles (water, impurities, etc.) promoting species with an uncoordinated dangling arm were ruled out since the rate of interconversion between isomers displays no concentration dependence and therefore the rearrangement seems to be intramolecular in nature.

### 2.2.2. Acyl complexes

The $^1$H-NMR spectra of acyl complexes [PdCl(COMe)(R′N–SR)] are characterised by a down-field shift of the signal ascribed to $COCH_3$ protons ($\Delta\delta \approx 1.5$ ppm with respect to methyl analogs). This evidence coupled with an intense IR signal at $\approx 1700$ cm$^{-1}$ testifies the CO insertion into the Pd–C bond [4d,15,16]. Since CO insertion takes place with retention of configuration [4d,15] we postulate that the acyl complexes would display the customary N–COMe *trans* configuration (vide supra). The reduced basicity of the acyl with respect to the methyl group indeed will explain the absence of the ancillary ligand rotation even in the 6-chloropyridine acyl complexes, owing to the increased electrophilicity of the metal core which would render the Pd–nitrogen bond more stable.

### 2.2.3. Allyl complexes

The complete characterisation of allyl complexes was achieved by studying authentic samples obtained via direct synthesis in $CH_2Cl_2$ between the suitable pyridylthioether R′N–SR ligand and the appropriate allyl dimer [Pd($\eta^3$-allyl)Cl]$_2$. However, the addition of DMA or TMA to a solution of [PdCl(Me)(R′N–SR)] or [PdCl(COMe)(R′N–SR)] substrates yields, upon addition of $NaClO_4$, the same allyl complexes. Therefore this path might represent a valid alternative route to the sterically hindered allyl species, [1,17] thereby overcoming the difficulties usually encountered when employing allene insertion methods [18]. The solution behaviour of the allyl complexes is conveniently studied by $^1$H-NMR technique since similar species had been investigated in depth and the resulting spectral features are well known [9c]. It would be useful to differentiate the studied allyl complexes on the basis of the allyl fragment symmetry. The complexes bearing the unsymmetrical allyl moiety would give rise to four diastereoisomers (together with their enantiomers which are undetectable under our experimental conditions). A topological representation of the diastereoisomers and the fluxional rearrangements involved at room temperature are given in the following scheme:

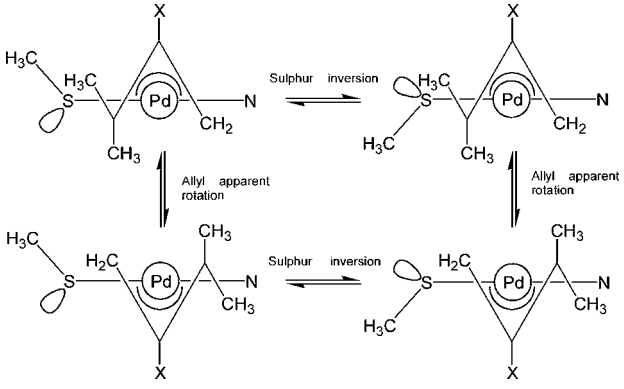


In fact in the room temperature $^1$H-NMR spectra of these complexes the presence of a sharp singlet ascribable to $CH_2S$ protons and of two couples of singlets attributed to *syn* and *anti* allyl $CH_3$ groups and protons, respectively, indicates the concomitant occurrence of both fluxional rearrangements (i.e. sulphur inversion and apparent rotation). No hints of *syn–anti* isomerism ($\eta^3$-$\eta^1$-$\eta^3$ rearrangement) are detectable at room temperature except for the cases of allyl–acyl complexes in which the collapse of the signals due to the allyl protons only suggests an operative and selective *syn–anti* isomerism. On decreasing the temperature the apparent

rotation is suddenly 'frozen' but the sulphur inversion phenomenon results still operative, albeit being by far the less energetic process [9c]. Only in the case of the −90 °C $CD_2Cl_2$ spectrum of the complex [Pd($\eta^3$-1,1,2-$Me_3C_3H_2$)(ClN–SMe)]$ClO_4$ together with the slightly broadened signals indicating the presence of two isomers (at different concentration) does a hint of only one AB quartet due to thioetheric protons of the less concentrated isomer become visible in the 4.1–4.5 ppm interval.

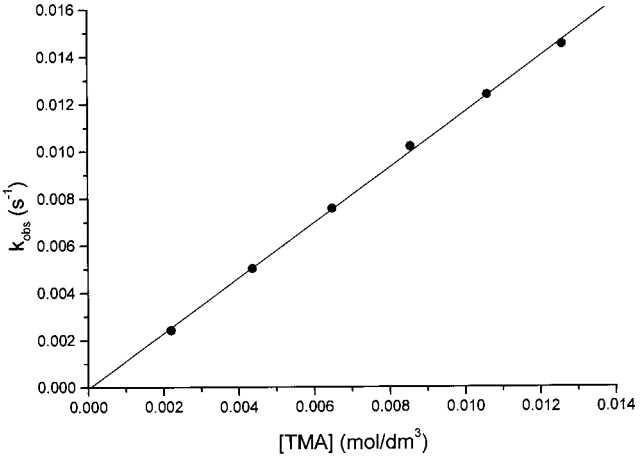


Fig. 3. Plot of $k_{obs}$ vs. [TMA] for the reaction of insertion of 1,1,3,3-tetramethylpropadiene (TMA) into the Pd–Me bond of the complex [PdCl(Me)(ClN-SMe)] in $CH_2Cl_2$ at 25 °C.

Table 2
Second-order rate constants, $k_2$ ($mol^{-1}$ $dm^3$ $s^{-1}$) for the insertion of 1,1-dimethylpropadiene (DMA) and 1,1,3,3-tetramethylpropadiene (TMA) across the Pd–Me and Pd–COMe bonds according to Eq. (2) in $CD_2Cl_2$ or $CH_2Cl_2$ at 25 °C

| Complexes | DMA | TMA |
|---|---|---|
| [PdCl(Me)(HN–SMe)] | $8.17 \times 10^{-4}$ [a] | [d] |
| [PdCl(Me)(HN–SEt)] | $6.53 \times 10^{-4}$ [a] | [d] |
| [PdCl(Me)(HN–S$^i$Pr)] | $4.08 \times 10^{-4}$ [a] | [d] |
| [PdCl(Me)(HN–S$^t$Bu)] | $2.33 \times 10^{-4}$ [a,c,b] | [d] |
| [PdCl(Me)(HN–SPh)] | $(4.0 \pm 0.3) \times 10^{-2}$ [b,c] | [d] |
| [PdCl(Me)(MeN–S$^t$Bu)] | $(3.3 \pm 0.1) \times 10^{-1}$ [b,c] | $(1.07 \pm 0.05) \times 10^{-2}$ [b,c] |
| [PdCl(Me)(MeN–SPh)] | $23 \pm 1$ [b,c] | $(4.6 \pm 0.1) \times 10^{-1}$ [b,c] |
| [PdCl(Me)(ClN–SMe)] | $117 \pm 25$ [e] | $1.18 \pm 0.07$ [c] |
| [PdCl(Me)(ClN–S$^t$Bu)] | $30 \pm 1$ [c] | $0.278 \pm 0.005$ [c] |
| [PdCl(Me)(ClN–SPh)] | $164 \pm 7$ [e] | $3.26 \pm 0.06$ [c] |
| [PdCl(COMe)(HN–S$^t$Bu)] | $(1.37 \pm 0.07) \times 10^{-2}$ [c] | – |
| [PdCl(COMe)(MeN–S$^t$Bu)] | $1.27 \pm 0.07$ [c] | $(8.7 \pm 0.3) \times 10^{-3}$ [c] |
| [PdCl(COMe)(ClN–S$^t$Bu)] | $160 \pm 10$ [e] | $1.93 \pm 0.09$ [c] |

[a] Measured by $^1$H-NMR technique in $CD_2Cl_2$ (see Section 2).
[b] Ref. [1].
[c] Measured by UV–vis technique in $CH_2Cl_2$ under pseudo-first order conditions.
[d] Too slow to measure.
[e] Measured by UV–vis technique in $CH_2Cl_2$ under second-order conditions.

The $^1$H-NMR spectra of the complexes bearing a symmetric allyl moiety are trivial and can be traced back to the customary features discussed elsewhere [19]. Again, no traces of $\eta^3$-$\eta^1$-$\eta^3$ isomerism due to steric hindrance of the allyl fragment are detected at room temperature.

### 2.3. Kinetics of allene insertion

The course of insertion of DMA (reaction 1) was monitored by $^1$H-NMR by following the disappearance of Pd–$CH_3$ proton signals at ~1 ppm in $CD_2Cl_2$ for the complexes [PdCl(Me)(HN–SR)] (R = Me, Et, *i*-Pr, *t*-Bu). The analogous insertion of TMA was too slow to measure due to product decomposition. The $k_2$ constants were computed from the resulting first half-lives under second-order conditions {$[Pd]_0 = 5 \times 10^{-2}$, $[DMA]_0 = 0.25$ mol $dm^{-3}$; $k_2 = \ln((2[DMA]_0 - [Pd]_0)/[DMA]_0)/t_{1/2}([DMA]_0 - [Pd]_0)$}.

The faster reactions were followed by UV–vis technique at 25 °C in $CH_2Cl_2$ under pseudo-first order conditions ($[A]_0 \geq 10 \times [Pd]_0$), ($[Pd]_0 \approx 1 \times 10^{-4}$ mol $dm^{-3}$) or second-order conditions for the fastest ones. For the former, the $k_2$ values were determined as the slopes of plots of pseudo-first order rate constants, $k_{obs}$, versus $[A]_0$, according to rate law (2) (A = allene) (Fig. 3):

$$k_{obs} = k_2[A]_0 \quad (2)$$

The $k_{obs}$ values were determined by non-linear fitting of absorbance data ($D$) to time according to the first-order monoexponential law $D_t = D_\infty + (D_0 - D_\infty)\exp(-k_{obs}t)$.

In no case could a statistically significant intercept be detected, corresponding to an allene-independent path, at variance with what was observed previously for the insertion of norbornadiene and allene into the palladium–carbon bond of complexes containing bidentate nitrogen ligands [4e,g,i].

For the faster reactions under second-order conditions ($[Pd]_0 \approx 1 \times 10^{-4}$, $[A]_0 \approx 1$–$5 \times 10^{-4}$ mol $dm^{-3}$) the $k_2$ constants were directly determined by non-linear regression of absorbance data to the customary second-order integrated rate law.

As can be seen from the data in Table 2, the following effects on the rate can be assessed:

(i) Steric hindrance at the allene moiety depresses dramatically the rate of insertion to the extent that the more hindered TMA does not lend itself to a kinetic study with complexes bearing HN–SR (R = Me, Et, *i*-Pr, *t*-Bu, Ph) as ancillary ligands.
(ii) Increasing steric hindrance at the sulphur substituent R depresses the rate to some extent (less than one order of magnitude); a phenyl group, which displays steric properties similar to those of *i*-Pr, imparts a marked rate increase (two orders of magnitude).

(iii) The presence of a substituent in the position 6 of the pyridine ring (R′ = Me, Cl) causes a striking increase in rate. The highest effect is reached when both R′ and R are good electron-attracting groups (R′ = Cl; R = Ph).
(iv) Other things being equal, acyl–palladium complexes react much faster with DMA than their methyl–palladium analogs.
(v) These reactivity trends are also effective in the reactions involving TMA, albeit with much lower rates.

These findings are in agreement with a simple stepwise mechanism involving formation of an intermediate adduct containing the starting metal substrate and the coordinated allene (**I**), followed by migration of the X group to yield the allene insertion product **2** according to the following scheme:

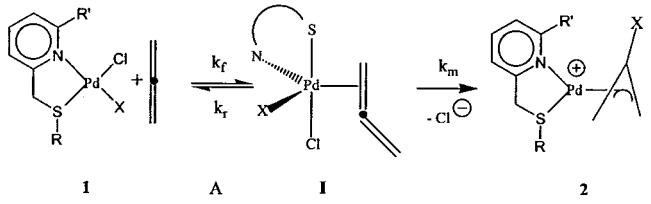


1 A I 2

In this mechanistic framework, under the assumption of steady-state conditions for [**I**] the second-order rate constant in Eq. (2) is to be read as

$$k_2 = k_f k_m/(k_r + k_m) \quad (3)$$

where $k_f$ is the second-order rate constant for bimolecular associative formation of **I**, $k_r$ is the first-order rate constant for monomolecular dissociation of **I** back to starting reactants, $k_m$ is the first-order rate constant for monomolecular migration of X to the allene moiety.

We can only provide a stoichiometric indication of the nature of intermediate **I** as a five-coordinate adduct since it could never be detected. Alternative formulations might involve either a four-coordinate species containing a monodentate R′N–SR ligand with a dangling uncoordinated arm or a cationic chelate form of the type $[Pd(\eta^2\text{-allene})(X)(R'N–SR)]^+Cl^-$. However, the view of intermediate **I** as a five-coordinate species, while providing the simplest mechanistic picture based on the available experimental evidence, fits well in the well-established wealth of knowledge gathered so far in the field of nucleophilic substitution on square-planar $d^8$ metal complexes. As a matter of fact, formation of **I** is just a case of associative asynchronous bond making between the metal substrate and the allene as the nucleophile, with the migrating X group playing the role of the 'leaving group' [20]. In this picture, the allene, the X group, and the group *trans* to X will lie on the same plane (the equatorial positions of a trigonal bipyramid), thereby providing an easy route to insertion [21] (incidentally this would explain the higher reactivity of metal solvento-species compared to neutral ones toward insertion of small unsaturated molecules [3e]). Since there is no merit in invoking more complicated mechanisms than those required by the experimental evidence, we are reluctant to entertain other possible mechanistic hypotheses involving the role of solvento-species or intermediate isomerisation steps [4c,4g,15] on the basis of the rate law (2) found experimentally in our system.

As a matter of fact, the rate of bimolecular association, $k_f$, is expected to be depressed by increased steric hindrance at both the entering allene (TMA vs. DMA) and the sulphur substituent R, the effect being, however, overwhelmed if R is an electron-accepting group such as Ph which will increase the electrophilic character of the metallic center and will render it more prone to allene association. Moreover, steric hindrance will also increase the rate of intermediate reversal to starting reactants, thereby producing the observed overall decrease in reactivity.

Furthermore, substitution at the 6-position of the pyridine ring, which has been shown to provoke severe distortion of the substrate's main coordination plane, [1] will cause a remarkable rate enhancement due to destabilisation of the ground state and a concomitant increase in the $k_f$ constant.

The presence of a 6-methyl substituent in the pyridine ring of a pyridyl–phosphine ligand bound to Pd(II) has been shown to enhance markedly the rate and the selectivity of methoxy carbonylation of propyne catalysed by such palladium(II) complexes [22]. Substituents adjacent to the nitrogen donor atom in bidentate α-diimine methylpalladium(II) complexes also were shown to strongly accelerate carbon monoxide insertion into the Pd–Me bond [4e]. These effects can be attributed to the ensuing distortion from planarity of the coordination environment (vide supra), causing a greater tendency to form five-coordinate complexes with unsaturated species [23]. However, the acceleration effects by pyridine 6-substituents that we have found here (Table 3) are *by far the greatest observed* since all these precedents, indicating that the flexible structure of our S-donor chelate R′N–SR ligands is particularly suited to exploit these effects, since it will allow severe distortion while imparting sufficient stability to the metal–polydentate ligand framework, thereby preventing decomposition of the substrate in the course of allene insertion. The effect is, expectedly, magnified by increased electron-withdrawing properties of the 6-substituent (e.g. Cl), which will make the metal center even more electrophilic toward allene association. This would also hold true if intermediate **I** is a four-coordinate species with a dangling N-arm, since the electronegative 6-chloride would depress the coordinating capability of the pyridine nitrogen and labilise the bidentate R′N–SR ligand.

Table 3
$^1$H- and $^{13}$C-NMR data for the complexes at 25 °C in $CDCl_3$

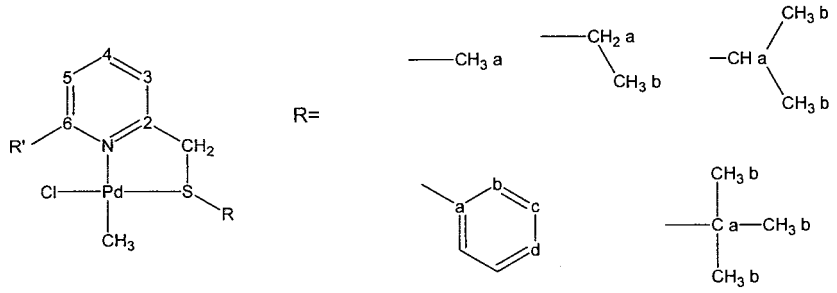


$^1$H NMR

| | R' | H$^3$ | H$^4$ | H$^5$ | S-C<u>H</u>$_2$ | Pd-C<u>H</u>$_3$ | R |
|---|---|---|---|---|---|---|---|
| R'=H R=Me | d 9.21 J=5.2 Hz | d 7.47 J=7.8 Hz | td 7.81 J=7.8 Hz J=1.7 Hz | dd 7.38 J=7.8 Hz J=5.2 Hz | bs 4.28 | s 0.86 | s 2.45 (a) |
| R'=H R=Et | d 9.20 J=5.0 Hz | d 7.45 J=7.8 Hz | td 7.80 J=7.8 Hz J=1.7 Hz | dd 7.38 J=7.8 Hz J=5.0 Hz | bs 4.27 | s 0.86 | q 2.77 (a) J=7.4 Hz t 1.39 (b) J=7.4 Hz |
| R'=H R=*i*-Pr | d 9.20 J=5.2 Hz | d 7.46 J=7.8 Hz | td 7.69 J=7.8 Hz J=1.7 Hz | dd 7.35 J=7.8 Hz J=5.2 Hz | bs 4.25 | s 0.88 | sept 3.01 (a) J=6.8 Hz d 1.37 (b) J=6.8 Hz |
| R'=H R=*t-Bu* | d 9.21 J=5.1 Hz | d 7.45 J=7.8 Hz | td 7.69 J=7.8 Hz J=1.7 Hz | dd 7.34 J=7.8 Hz J=5.1 Hz | bs 4.27 | s 0.92 | s 1.34 (b) |
| R'=H R=Ph | d 9.29 J=5.0 Hz | 7.58 unresolv. | 7.58 unresolv. | 7.58 unresolv. | bs 4.52 | s 0.91 | m 7.58 (b,c,d) |
| R'=Me R=*t-Bu* | s 3.08 | d 7.19 J=7.7 Hz | t 7.61 J=7.7 Hz | d 7.14 J=7.7 Hz | AB sys 4.61, 4.14 J=17.2 Hz | s 1.12 | s 1.25 (a) |
| R'=Me R=Ph | s 3.10 | d 7.12 J=7.7 Hz | t 7.52 J=7.7 Hz | d 7.02 J=7.7 Hz | bs 4.61 | s 1.14 | m 7.63 (c) m 7.33 (b,d) |
| R'=Cl R=Me | - | d 7.33 J=7.7 Hz | t 7.73 J=7.7 Hz | d 7.60 J=7.7 Hz | s 4.18 | s 0.88 | s 2.40 (a) |
| R'=Cl R=*t-Bu* | - | d 7.35 J=7.7 Hz | t 7.69 J=7.7 Hz | bs 7.4 | br AB sys 4.51 4.23 | s 1.16 | s 1.31 (b) |
| R'=Cl R=Ph | - | bd 7.16 | t 7.59 J=7.8 Hz | bs 7.76 | bs 4.55 | s 1.03 | m 7.33 (b,c,d) |

$^{13}$C {$^1$H} NMR

| | R' | C$^2$ | C$^3$ | C$^4$ | C$^5$ | C$^6$ | S-C<u>H</u>$_2$ | Pd-C<u>H</u>$_3$ | R |
|---|---|---|---|---|---|---|---|---|---|
| R'=H R=Me | - | 155.5 | 123.9 | 138.2 | 123.2 | 150.5 | 46.0 | -9.7 | 21.9 (a) |
| R'=H R=Et | - | 156.1 | 123.8 | 138.1 | 122.7 | 150.4 | 43.5 | -10.2 | 32.5 (a) 13.9 (b) |
| R'=H R=*i*-Pr | - | 156.5 | 123.7 | 138.2 | 122.3 | 150.4 | 42.2 | -10.2 | 42.1 (a) 23.2 (b) |
| R'=H R=*t-Bu* | - | 157.2 | 123.5 | 128.3 | 121.7 | 150.1 | 41.4 | -9.6 | 51.2 (a) 30.2 (b) |
| R'=H R=Ph | - | 155.7 | 123.9 | 138.2 | 122.6 | 150.3 | 50.1 | -5.6 | 131.0 (a) 129.7 (b) 132.8 (c) 130.5 (d) |
| R'=Me R=*t*-Bu | 26.6 | 162.5 | 124.6 | 138.0 | 119.2 | 151.0 | 42.0 | -5.6 | 50.0 (a) 30.2 (b) |
| R'=Me R=Ph | 26.5 | 162.7 | 120.3 | 138.0 | 120.4 | 154.3 | 49.6 | -4.6 | 129.5 (b) 132.9 (c) 130.2 (d) |
| R'=Cl R=Me | - | 155.5 | 122.8 | 139.4 | 123.7 | 151.2 | 43.6 | 0.23 | 19.7 (a) |
| R'=Cl R=*t*-Bu | - | 157.0 | 120.9 | 139.7 | 125.0 | 153.3 | 40.5 | -5.1 | 50.3 (a) 30.1 (b) |
| R'=Cl R=Ph | - | 155.4 | 122.1 | 139.2 | 124.1 | 152.0 | 46.5 | -0.69 | 131.8 (a) 129.2 (b) 132.7 (c) 129.8 (d) |

Table 3 (*Continued*)

*Acyl complexes*

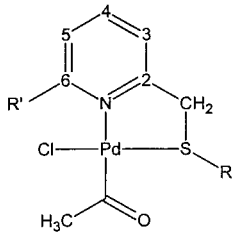


$^{1}$H NMR

| | R' | H$^{3}$ | H$^{4}$ | H$^{5}$ | S-C$\underline{H}_2$ | CO-C$\underline{H}_3$ | R |
|---|---|---|---|---|---|---|---|
| R'=H R=*t*-Bu | d 9.02 J=5.4 Hz | d 7.25 J=7.8 Hz | td 7.79 J=7.8 Hz J=1.7 Hz | dd 7.34 J=7.8 Hz J=5.4 Hz | bs 4.27 | s 2.62 | s 1.37 (b) |
| R'=Me R=*t*-Bu | s 3.01 | d 7.16 J=7.7 Hz | t 7.60 J=7.7 Hz | d 7.12 J=7.7 Hz | s 4.40 | s 2.64 | s 1.25 (b) |
| R'=Cl R=*t*-Bu | - | d 7.35 J=7.8 Hz | t 7.73 J=7.7 Hz | d 7.41 J=7.7 Hz | s 4.35 | s 2.59 | s 1.34 (b) |

$^{13}$C {$^{1}$H} NMR

| | R' | C$^{2}$ | C$^{3}$ | C$^{4}$ | C$^{5}$ | C$^{6}$ | S-C$\underline{H}_2$ | C$\underline{O}$ | CO-C$\underline{H}_3$ | R |
|---|---|---|---|---|---|---|---|---|---|---|
| R'=Cl R=*t*-Bu | - | 156.2 | 121.1 | 139.9 | 125.9 | 156.2 | 39.8 | 174.2 | 36.0 | 50.9 (a) 30.3 (b) |

*Allyl Complexes*

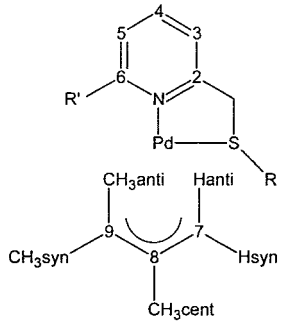


$^{1}$H NMR

| | R' | H$^{3}$ | H$^{4}$ | H$^{5}$ | S-C$\underline{H}_2$ | R | H syn | H anti | C$\underline{H}_3$ cent | C$\underline{H}_3$ syn | C$\underline{H}_3$ anti |
|---|---|---|---|---|---|---|---|---|---|---|---|
| R'=H R=Me | bs 8.73 | d 7.81 7.7 Hz | t 7.97 7.7 Hz | bs 7.48 | bs 4.48 | s 2.49 (a) | s 4.18 | s 3.87 | s 2.18 | s 1.76 | s 1.48 |
| R'=H R=Et | bs 8.64 | d 7.82 7.7 Hz | t 7.97 7.8 Hz | bs 7.49 | bs 4.48 | q 2.49 (a) 7.7 Hz t 1.35 (b) 7.7 Hz | s 4.26 | s 3.95 | s 2.18 | s 1.76 | s 1.49 |
| R'=H R=*i*-Pr | m 8.73 | m 7.87 | m 7.97 | m 7.48 | bs 4.47 | m 3.20 (a) d 1.36 (b) | s 4.28 | s 3.96 | s 2.18 | s 1.77 | s 1.51 |
| R'=H R=*t*-Bu | m 8.74 | bd 7.85 unresolv. | s 7.97 unresolv. | bd 7.48 7.7 Hz | bs 4.47 | s 1.35 (b) | s 4.26 | s 3.95 | s 2.18 | s 1.76 | s 1.49 |

Table 3 (*Continued*)

| | | | | | | | | | | | |
|---|---|---|---|---|---|---|---|---|---|---|---|
| R'=H R=Ph | bs 8.88 | d 7.66 7.7 Hz | td 7.92 7.7 Hz 1.6 Hz | m 7.47 unresolv. | bs 4.76 | m 7.47 (b,c,d) | s 4.35 | s 4.02 | s 2.18 | s 1.61 | s 1.33 |
| R'=Me R=*t*-Bu | s 3.76 | d 7.65 7.7 Hz | t 7.97 7.7 Hz | s 7.36 7.7 Hz | bs 4.51 | s 1.26 (a) | s 4.45 | s 3.76 | s 2.16 | s 1.75 | s 1.50 |
| R'=Me R=Ph | s 2.81 | m 7.42 unresolv. | t 7.73 7.7 Hz | m 7.42 unresolv. | s 4.82 | m 7.42 (b,c,d) | s 4.57 | s 3.94 | s 2.21 | s 1.65 | s 1.42 |
| R'=Cl R=Me | - | d 7.57 7.7 Hz | t 7.96 7.7 Hz | d 7.81 7.7 Hz | s 4.58 | s 2.40 (a) | s 4.63 | s 3.95 | s 2.17 | s 1.70 | s 1.45 |
| R'=Cl R=*t*-Bu | - | d 7.54 7.7 Hz | t 7.97 7.7 Hz | d 7.90 7.7 Hz | AB sys 4.56, 4.68 J=17.9 Hz | s 1.30 (b) | s 4.65 | s 3.95 | s 2.17 | s 1.72 | s 1.49 |
| R'=Cl R=Ph | - | d 7.48 7.8 Hz | m 7.48 unresolv. | m 7.85 unresolv. | s 4.91 | m 7.48 (b,c,d) | s 4.76 | s 4.10 | s 2.22 | s 1.65 | s 1.42 |

$^{13}C\{^1H\}$ NMR

| | R' | $C^2$ | $C^3$ | $C^4$ | $C^5$ | $C^6$ | S-$CH_2$ | R | $C^7$ | $C^8$ | $C^9$ | $CH_3$ cent | $CH_3$ syn | $CH_3$ anti |
|---|---|---|---|---|---|---|---|---|---|---|---|---|---|---|
| R'=Cl R=Me | - | 159.8 | 124.5 | 142.0 | 125.2 | 152.7 | 42.9 | 18.2 (a) | 69.9 | 125.9 | 88.9 | 25.0 | 24.5 | 20.6 |
| R'=Cl R=*t*-Bu | - | 161.2 | 123.3 | 142.3 | 124.7 | 152.0 | 39.85 | 50.7 (a) 30.6 (b) | 69.7 | 126.0 | 89.6 | 25.6 | 24.5 | 20.7 |
| R'=Cl R=Ph | - | 159.5 | 123.7 | 141.9 | 124.9 | 152.3 | 25.1 | 126.3 (a) 131.9 (b) 130.0 (c) 130.3 (d) | 70.6 | 124.9 | 90.3 | 25.1 | 24.5 | 20.5 |

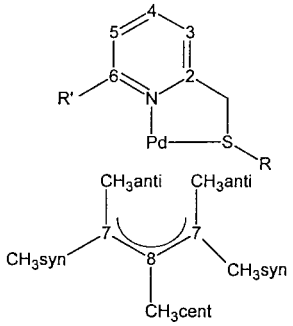


$^1H$ NMR

| | R' | $H^3$ | $H^4$ | $H^5$ | S-$CH_2$ | R | $CH_3$ cent | $CH_3$ syn | $CH_3$ anti |
|---|---|---|---|---|---|---|---|---|---|
| R'=Me R=*t*-Bu | s 2.83 | d 7.64 7.7 Hz | t 7.83 7.7 Hz | d 7.43 7.7 Hz | bs 4.48 | s 1.21 (a) | s 2.10 | s 1.82 | s 1.75 |
| R'=Me R=Ph | s 2.84 | m 7.35 unresolv. | t 7.67 7.7 Hz | m 7.35 unresolv. | bs 4.78 | m 7.35 (b,c,d) | s 2.17 | s 1.86 | s 1.79 |
| R'=Cl R=Me | - | d 7.53 7.7 Hz | t 7.94 7.7 Hz | d 7.79 7.7 Hz | s 4.48 | s 2.26 (a) | s 2.09 | s 1.82 | s 1.76 |
| R'=Cl R=*t*-Bu | - | d 7.51 7.7 Hz | t 7.95 7.7 Hz | d 7.88 7.7 Hz | s 4.55 | s 1.25 (b) | s 2.10 | s 1.83 | s 1.77 |
| R'=Cl R=Ph | - | m 7.44 unresolv. | t 7.78 7.8 Hz | d 7.56 7.8 Hz | s 4.48 | m 7.44 (b,c,d) | s 2.18 | s 1.87 | s 1.81 |

$^{13}C\{^1H\}$ NMR

| | R' | $C^2$ | $C^3$ | $C^4$ | $C^5$ | $C^6$ | S-$CH_2$ | R | $C^7$ | $C^8$ | $CH_3$ cent | $CH_3$ syn | $CH_3$ anti |
|---|---|---|---|---|---|---|---|---|---|---|---|---|---|
| R'=Cl R=Me | - | 159.1 | 125.0 | 141.7 | 125.0 | 152.5 | 42.5 | 17.4 (a) | 92.0 | 119.6 | 29.6 | 27.2 | 19.0 |
| R'=Cl R=*t*-Bu | - | 160.6 | 123.7 | 142.0 | 124.8 | 15.7 | 39.7 | 49.7(a) 30.6 (b) | 91.5 | 120.2 | 29.7 | 27.4 | 19.2 |
| R'=Cl R=Ph | - | 158.8 | 123.7 | 141.7 | 124.3 | 151.9 | 46.1 | 124.7 (a) 129.8 (b) 132.1 (c) 130.0 (d) | 70.6 | 124.9 | 29.6 | 27.5 | 19.2 |

Table 3 (*Continued*)

*Acyl-allyl complexes*

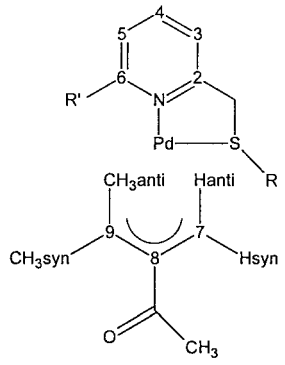


$^1$H NMR

| | R' | H$^3$ | H$^4$ | H$^5$ | S-C$\underline{H}_2$ | R | H syn | H anti | CO-C$\underline{H}_3$ | C$\underline{H}_3$ syn | C$\underline{H}_3$ anti |
|---|---|---|---|---|---|---|---|---|---|---|---|
| R'=H R=*t*-Bu | d 8.68 7.7 Hz | d 7.87 7.7 Hz | td 7.97 7.7 Hz 1.4 Hz | td 7.51 7.7 Hz 1.4 Hz | s 4.53 | s 1.35 | bs 4.05 | bs 4.05 | s 2.50 | s 1.79 | s 1.60 |
| R'=Me R=*t*-Bu | s 2.76 | d 7.61 7.7 Hz | t 7.83 7.7 Hz | d 7.37 7.7 Hz | bs 4.59 | s 1.24 | bs 4.07 | bs 4.07 | s 2.50 | s 1.75 | s 1.59 |
| R'=Cl R=*t*-Bu | - | d 7.54 7.6 Hz | t 7.96 7.6 Hz | d 7.85 7.6 Hz | bs 4.69 | s 1.30 | s 4.47 | s 3.08 | s 2.53 | s 1.72 | s 1.56 |

$^{13}$C {$^1$H} NMR

| | R' | C$^2$ | C$^3$ | C$^4$ | C$^5$ | C$^6$ | S-C$\underline{H}_2$ | R | C$^7$ | C$^8$ | C$^9$ | CO-C$\underline{H}_3$ | C$\underline{H}_3$ syn | C$\underline{H}_3$ anti |
|---|---|---|---|---|---|---|---|---|---|---|---|---|---|---|
| R'=H R=*t*-Bu | - | 160.3 | 124.2 | 140.2 | 124.8 | 153.0 | 39.4 | 51.4 (a) 30.4 (b) | 60.0 | 126.4 | 90.0 | 29.4 | 23.6 | 23.6 |
| R'=Me R=*t*-Bu | 29.7 | 159.8 | 121.4 | 140.2 | 124.4 | 159.8 | 40.1 | 51.1 (a) 30.5 (b) | 62.2 | 126.7 | 91.0 | 29.5 | 25.8 | 23.6 |
| R'=Cl R=*t*-Bu | - | 161.3 | 123.2 | 142.3 | 124.7 | 151.9 | 39.7 | 50.7 (a) 30.6 (b) | 65.5 | 56.17 | 91.8 | 29.4 | 26.0 | 23.9 |

The fact that the acyl complexes react faster than their methyl analogs (Table 2) has already been observed with bidentate nitrogen ligands [4g], and is likely to stem from faster allene association to the metal, due to the lower basicity of COMe relative to Me which should favour formation of the electron-rich species **I**, although this factor would be expected to disfavour the migratory insertion step. Apparently, the balance of these contrasting effects results in a much faster overall rate. The rate increase on going from X = Me to X = COMe is much less marked with substituted 6-pyridine ring ligands (R′ = Me, Cl), owing to a levelling-off effect on the reactivity of the starting substrates. With the sterically hindered allene TMA the reactivities of the methyl and acetyl complexes are of the same order of magnitude, suggesting that steric hindrance to allene association leads to limiting values in the rates.

## 3. Experimental

### 3.1. Synthesis of ligands

#### 3.1.1. 6-Chloro-2-chloromethylpyridine

The title compound was prepared according to published procedure by reacting $SOCl_2$ with (6-chloropyridin-2-yl)-methanol [24], which was obtained from the commercially available 2-chloro-6-methylpyridine following the method reported by Chi and co-workers [25].

#### 3.1.2. 6-Chloro-2-methylthiomethylpyridine (ClN–SMe)

To a solution of 2.77 g (49.38 mmol) of KOH in 20 ml of DMSO, 0.865 g (12.34 mmol) of $CH_3S^-Na^+$ and 1.0 g (6.17 mmol) of 6-chloro-2-chloromethylpyridine were added. The resulting solution was stirred for 1.5 h at room temperature (r.t.) 60 ml of water was then added. The product was extracted with $Et_2O$ (120 ml) and the resulting solution was treated with anhydrous $Na_2SO_4$ (12 h), filtered and dried under vacuum. The crude yellowish oil was purified by flash-chromatography ($SiO_2$) using *n*-hexane–$Et_2O$ 9:1 v/v as eluent. 0.482 g (2.78 mmol) of the title product was obtained. In this case the attack of excess $CH_3S^-$ at the aromatic ring yields 6-thiomethyl-2-methylthiomethylpyridine in large quantity (yield 40%; identified from its $^1$H-NMR spectrum: $\delta$ (ppm) 2.65 (S–C$H_3$, s, 3H); 3.75 (C$H_2$–S–CH$_3$, s, 2H); 2.11 (CH$_2$–S–C$H_3$, s, 3H); 7.03 ($H^3_{(pyr)}$, d, $J = 8.0$ Hz, 1H); 7.05 ($H^5_{(pyr)}$, d, $J = 8.0$ Hz, 1H); 7.47 ($H^4_{(pyr)}$, t, $J = 8.0$ Hz, 1H)).

Yield: 45%. Found: C, 48.52; H, 4.61; N, 7.98. $C_7H_8NSCl$ requires: C, 48.41; H, 4.64; N, 8.07%. IR

(KBr, $cm^{-1}$) $\nu_{C=N}$ 1582(s). $^1$H-NMR ($CDCl_3$): $\delta$ (ppm) 2.08 (S–C$H_3$, s, 3H); 3.76 (C$H_2$–S, s, 2H); 7.22 ($H^5_{(pyr)}$, d, $J = 7.7$ Hz, 1H); 7.32 ($H^3_{(pyr)}$, d, $J = 7.7$ Hz, 1H); 7.64 ($H^4_{(pyr)}$, t, $J = 7.7$ Hz, 1H). $^{13}$C-NMR ($CDCl_3$): $\delta_{(ppm)}$ 15.2 (S–$CH_3$); 39.4 (S–$CH_2$); 121.3 ($C^3_{(pyr)}$); 121.4 ($C^5_{(pyr)}$); 139.2 ($C^4_{(pyr)}$); 150.6 ($C^6_{(pyr)}$); 159.7 ($C^2_{(pyr)}$).

The following compounds were prepared similarly to the above described ClN–SMe ligand using the appropriate thiolate species.

*3.1.3. 6-Chloro-2-tert-butylthiomethylpyridine (ClN–S–$^t$Bu)*

Yield: 94%. Found: C, C, 55.58; H, 6.60; N, 6.48. $C_{10}H_{14}NSCl$ requires: C, 55.67; H, 6.54; N, 6.49%. IR (KBr, $cm^{-1}$) $\nu_{C=N}$ 1583.5(s). $^1$H-NMR ($CDCl_3$): $\delta$ (ppm) 1.32 (C–C$H_3$, s, 9H); 3.87 (C$H_2$–S, s, 2H); 6.96 ($H^5_{(pyr)}$, d, $J = 7.7$ Hz, 1H); 7.21 ($H^3_{(pyr)}$, d, $J = 7.7$ Hz, 1H); 7.49 ($H^4_{(pyr)}$, t, $J = 7.7$ Hz, 1H). $^{13}$C-NMR ($CDCl_3$): $\delta$ (ppm) 30.7 (C($CH_3$)$_3$); 34.8 (S–$CH_2$); 43.1 ($C$(CH$_3$)$_3$); 121.5 ($C^3_{(pyr)}$); 121.9 ($C^5_{(pyr)}$); 138.8 ($C^4_{(pyr)}$); 150.1 ($C^6_{(pyr)}$); 160.3 ($C^2_{(pyr)}$).

*3.1.4. 6-Chloro-2-phenylthiomethylpyridine (ClN–SPh)*

Yield: 90%. Found: C, 61.18; H, 4.31; N, 6.01. $C_{12}H_{10}NSCl$ requires: C, 61.14; H, 4.28; N, 5.94%. IR (KBr, $cm^{-1}$): $\nu_{C=N}$ 1584.6(s). $^1$H-NMR ($CDCl_3$): $\delta$ (ppm) 4.23 (C$H_2$–S, s, 2H); 7.26 ($H^{3,5}_{(pyr)} + H_{(phen)}$, m, 7H); 7.56 ($H^4_{(pyr)}$, t, $J = 7.7$ Hz, 1H). $^{13}$C-NMR ($CDCl_3$): $\delta$ (ppm) 39.7 (S–$CH_2$); 121.0 ($C^3_{(pyr)}$); 122.3 ($C^5_{(pyr)}$); 126.3 ($C^p_{(phen)}$); 128.7 ($C^o_{(phen)}$); 129.5 ($C^m_{(phen)}$); 135.0 (S–$C$); 138.9 ($C^4_{(pyr)}$); 150.4 ($C^6_{(pyr)}$); 158.5 ($C^2_{(pyr)}$).

*3.1.5. R′N–SR (R′ = H; R = Me, Et, i-Pr, t-Bu, Ph: R′ = Me; R = t-Bu, Ph)*

These pyridylthioether ligands were synthesised according to published procedures [5,9c].

*3.2. Synthesis of complexes*

*3.2.1. [PdCl(Me)(COD)]*

The title complex was obtained according to published procedure [26] by adding $Sn(Me)_4$ to a $CH_2Cl_2$ solution of [$PdCl_2$COD] [27] under inert atmosphere ($N_2$).

$^1$H- and $^{13}$C-NMR data for the new complexes reported in this section are summarised in Table 3.

*3.2.2. [PdCl(Me)(ClN–SMe)]*

To 198.1 mg (0.7475 mmol) of the complex [PdCl(Me)(COD)] dissolved in 30 ml of freshly distilled toluene, 142.8 mg (0.8223 mmol) of ClN–SMe ligand was added under inert atmosphere ($N_2$). The resulting solution was stirred at r.t. for 4 h and eventually dried under reduced pressure. The residue was dissolved in $CH_2Cl_2$, treated with activated charcoal and filtered on celite filter. Reduction to small volume and precipitation with *n*-hexane at 0 °C yields 215.5 mg (0.6519 mmol) of the title complex as pale-yellow microcrystals.

Yield: 87%. Found: C, 29.12; H, 3.31; N, 4.21. $C_8H_{11}NSCl_2Pd$ requires: C, 29.07; H, 3.35; N, 4.24%. IR (KBr, $cm^{-1}$): $\nu_{C=N}$ 1581.6(s).

The following complexes were prepared in the same way as [PdCl(Me)(ClN–SMe)] using the appropriate ligand.

*3.2.3. [PdCl(Me)(ClN–S$^t$Bu)] (pale-yellow microcrystals)*

Yield: 89%. Found: C, 34.51; H, 4.58; N, 3.81. $C_{11}H_{17}NSCl_2Pd$ requires: C, 35.46; H, 4.60; N, 3.76%. IR (KBr, $cm^{-1}$): $\nu_{C=N}$ 1583.5(s).

*3.2.4. [PdCl(Me)(ClN–SPh)] (pale-yellow microcrystals)*

Yield: 83%. Found: C, 39.82; H, 3.34; N, 3.60. $C_{14}H_{15}NSCl_2Pd$ requires: C, 39.77; H, 3.34; N, 3.57%. IR (KBr, $cm^{-1}$): $\nu_{C=N}$ 1589.3(s).

*3.2.5. [PdCl(Me)(HN–SMe)] (yellow microcrystals)*

Yield: 87%. Found: C, 32.41; H, 4.11; N, 4.71. $C_8H_{12}NSClPd$ requires: C, 32.45; H, 4.08; N, 4.73%. IR (KBr, $cm^{-1}$): $\nu_{C=N}$ 1601(s).

*3.2.6. [PdCl(Me)(HN–SEt)] (yellow microcrystals)*

Yield: 89%. Found: C, 34.90; H, 4.51; N, 4.53. $C_9H_{14}NSClPd$ requires: C, 34.86; H, 4.55; N, 4.52%. IR (KBr, $cm^{-1}$): $\nu_{C=N}$ 1601(s).

*3.2.7. [PdCl(Me)(HN–S–$^i$Pr)] (pale-yellow microcrystals)*

Yield: 85%. Found: C, 36.97; H, 5.01; N, 4.20. $C_9H_{16}NSClPd$ requires: C, 37.05; H, 4.97; N, 4.23%. IR (KBr, $cm^{-1}$): $\nu_{C=N}$ 1601(s).

The following complexes were prepared according to published procedure [1]. The used methods were, however, similar to those described above.

[PdCl(Me)(HN–S–t-Bu)] (yellow microcrystals);

[PdCl(Me)(HN–SPh)] (bright-yellow microcrystals);

[PdCl(Me)(MeN–S–t-Bu)] (pale-yellow microcrystals); and

[PdCl(Me)(MeN–SPh)] (pale-yellow microcrystals).

*3.2.8. [PdCl(COMe)(HN–S–$^t$Bu)]*

Gaseous carbon monoxide (CO) was bubbled through a stirred solution of 101.8 mg (0.301 mmol) of [PdCl(Me)(HN–S–$^t$Bu)] dissolved in 30 ml of freshly distilled $CH_2Cl_2$ for 1 h. The resulting solution was treated with activated charcoal filtered on celite filter and concentrated under reduced pressure. Addition of diethylether yields 93.2 mg (0.254 mmol) of the acyl complex as a pale-yellow solid.

Yield: 84%. Found: C, 39.37; H, 5.01; N, 3.92. $C_{12}H_{18}NOSClPd$ requires: C, 39.36; H, 4.95; N, 3.82%. IR (KBr, $cm^{-1}$): $\nu_{C=N}$ 1601(s); $\nu_{C=O}$ 1693(s).

The following complexes were prepared in the same way as [PdCl(COMe)(HN–S–$^t$Bu)] using the appropriate starting substrates.

*3.2.9. [PdCl(COMe)(MeN–S–$^t$Bu)] (pale-yellow microcrystals)*

Yield: 87%. Found: C, 40.97; H, 5.31; N, 3.72. $C_{13}H_{20}NOSClPd$ requires: C, 41.07; H, 5.30; N, 3.68%. IR (KBr, $cm^{-1}$): $\nu_{C=N}$ 1590(s); $\nu_{C=O}$ 1709(s).

*3.2.10. [PdCl(COMe)(ClN–S–$^t$Bu)] (whitish microcrystals, 79.0% yield)*

Yield: 84%. Found: C, 35.97; H, 4.25; N, 3.48. $C_{12}H_{17}NOSCl_2Pd$ requires: C, 35.98; H, 4.28; N, 3.50%. IR (KBr, $cm^{-1}$): $\nu_{C=N}$ 1585(s); $\nu_{C=O}$ 1715(s).

The following complexes were synthesised according to published procedures [4d].

$[Pd_2(\mu\text{-}Cl)_2(\eta^3\text{-}1,1,2\text{-}Me_3C_3H_2)_2]$ (pale-yellow microcrystals);

$[Pd_2(\mu\text{-}Cl)_2(\eta^3\text{-}1,1,2,3,3\text{-}Me_5C_3)_2]$ (pale-yellow microcrystals); and

$[Pd_2(\mu\text{-}Cl)_2(\eta^3\text{-}1,1\text{-}Me_2CC(COMe)CH_2)_2]$ (pale-yellow microcrystals).

*3.2.11. [Pd($\eta^3$-1,1,2-$Me_3C_3H_2$)(ClN–S–$^t$Bu)]$ClO_4$*

To a solution of 73.5 mg (0.163 mmol) of the dimer $[Pd_2(\mu\text{-}Cl)_2(\eta^3\text{-}1,1,2\text{-}Me_3C_3H_2)_2]$ in $CH_2Cl_2$ (2 ml), 74.6 mg (0.346 mmol) of the ligand ClN–S–$^t$Bu dissolved in 5 ml of $CH_2Cl_2$ and 94 mg (0.67 mmol) of $NaClO_4{\cdot}H_2O$ in 4 ml of MeOH were added. The cloudy solution was stirred at r.t. for 1 h and then dried under reduced pressure. The residue was dissolved in $CH_2Cl_2$, treated with activated charcoal and filtered on celite filter. The resulting solution was concentrated and treated with diethyl-ether. The allyl complex precipitated as a pale-yellow compound (155.6 mg, 0.308).

Yield: 94%. Found: C, 38.03; H, 4.96; N, 2.81. $C_{16}H_{25}NO_4SCl_2Pd$ requires: C, 38.07; H, 4.99; N, 2.78%. IR (KBr, $cm^{-1}$): $\nu_{C=N}$ 1585.5(s).

The following complexes were synthesised in the same way as [Pd($\eta^3$-1,1,2-$Me_3C_3H_2$)(ClN–S–$^t$Bu)]$ClO_4$ using the appropriate starting substrates and ligands.

*3.2.12. [Pd($\eta^3$-1,1,2-$Me_3C_3H_2$)(ClN–SMe)]$ClO_4$ (pale-yellow microcrystals)*

Yield: 91%. Found: C, 33.81; H, 4.16; N, 3.08. $C_{13}H_{19}NO_4SCl_2Pd$ requires: C, 33.75; H, 4.14; N, 3.03%. IR (KBr, $cm^{-1}$): $\nu_{C=N}$ 1584.6(s).

*3.2.13. [Pd($\eta^3$-1,1,2-$Me_3C_3H_2$)(ClN–SPh)]$ClO_4$ (pale-yellow microcrystals)*

Yield: 92%. Found: C, 41.17; H, 4.06; N, 2.72. $C_{18}H_{21}NO_4SCl_2Pd$ requires: C, 41.20; H, 4.03; N, 2.67%. IR (KBr, $cm^{-1}$): $\nu_{C=N}$ 1581.6(s).

*3.2.14. [Pd($\eta^3$-1,1,2,3,3-$Me_5C_3$)(ClN–SMe)]$ClO_4$ (pale-yellow microcrystals)*

Yield: 60%. Found: C, 36.67; H, 4.74; N, 2.82. $C_{15}H_{23}NO_4SCl_2Pd$ requires: C, 36.71; H, 4.72; N, 2.85%. IR (KBr, $cm^{-1}$): $\nu_{C=N}$ 1581.6(s).

*3.2.15. [Pd($\eta^3$-1,1,2,3,3-$Me_5C_3$)(ClN–S–$^t$Bu)]$ClO_4$ (pale-yellow microcrystals)*

Yield: 80%. Found: C, 43.51; H, 4.57; N, 2.51. $C_{18}H_{29}NO_4SCl_2Pd$ requires: C, 43.46; H, 4.56; N, 2.53%. IR (KBr, $cm^{-1}$): $\nu_{C=N}$ 1583.5(s).

*3.2.16. [Pd($\eta^3$-1,1,2,3,3-$Me_5C_3$)(ClN–SPh)]$ClO_4$ (pale-yellow microcrystals)*

Yield: 60%. Found: C, 43.48; H, 4.54; N, 2.55. $C_{20}H_{25}NO_4SCl_2Pd$ requires: C, 43.46; H, 4.56; N, 2.53%. IR (KBr, $cm^{-1}$): $\nu_{C=N}$ 1581.6(s).

*3.2.17. [Pd($\eta^3$-1,1-$Me_2CC(COMe)CH_2$)(ClN–S–$^t$Bu)]$ClO_4$ (pale-yellow microcrystals)*

Yield: 66%. Found: C, 36.03; H, 4.24; N, 3.48. $C_{17}H_{25}NO_5SCl_2Pd$ requires: C, 35.98; H, 4.28; N, 3.50%. IR (KBr, $cm^{-1}$): $\nu_{C=N}$ 1585.4(s); $\nu_{C=O}$ 1714.6(s).

*3.2.18. [Pd($\eta^3$-1,1-$Me_2CC(COMe)CH_2$)(HN–S–$^t$Bu)]$ClO_4$ (pale-yellow microcrystals)*

Yield: 56%. Found: C, 39.33; H, 4.97; N, 3.78. $C_{17}H_{26}NO_5SClPd$ requires: C, 39.36; H, 4.95; N, 3.82%. IR (KBr, $cm^{-1}$): $\nu_{C=N}$ 1601(s); $\nu_{C=O}$ 1693(s).

*3.2.19. [Pd($\eta^3$-1,1-$Me_2CC(COMe)CH_2$)(MeN–S–$^t$Bu)]$ClO_4$ (pale-yellow microcrystals)*

Yield: 59%. Found: C, 41.11; H, 5.28; N, 3.72. $C_{18}H_{28}NO_5SClPd$ requires: C, 41.07; H, 5.30; N, 3.68%. IR (KBr, $cm^{-1}$): $\nu_{C=N}$ 1590(s); $\nu_{C=O}$ 1709(s).

*3.2.20. [Pd($\eta^3$-1,1,2-$Me_3C_3H_2$)(HN–SMe)]$ClO_4$ (whitish microcrystals)*

Yield: 81%. Found: C, 36.43; H, 4.74; N, 3.25. $C_{13}H_{20}NO_4SClPd$ requires: C, 36.46; H, 4.71; N, 3.27%. IR (KBr, $cm^{-1}$): $\nu_{C=N}$ 1590(s).

*3.2.21. [Pd($\eta^3$-1,1,2-$Me_3C_3H_2$)(HN–SEt)]$ClO_4$ (whitish microcrystals)*

Yield: 93%. Found: C, 38.01; H, 4.97; N, 3.20. $C_{14}H_{22}NO_4SClPd$ requires: C, 38.02; H, 5.01; N, 3.17%. IR (KBr, $cm^{-1}$): $\nu_{C=N}$ 1601(s).

*3.2.22. [Pd($\eta^3$-1,1,2-$Me_3C_3H_2$)(HN–S–$^i$Pr)]$ClO_4$ (pale-yellow microcrystals)*

Yield: 99%. Found: C, 39.53; H, 5.34; N, 3.12. $C_{15}H_{24}NO_4SClPd$ requires: C, 39.49; H, 5.30; N, 3.07%. IR (KBr, $cm^{-1}$): $\nu_{C=N}$ 1603(s).

The following complexes were synthesised according to published procedures [1].

Table 4
Crystal data and structure refinement parameters

| | |
|---|---|
| Empirical formula | $C_8H_{12}ClNPdS$ |
| Formula weight | 296.1 |
| Crystal system | orthorhombic |
| Space group | $Pna2_1$ (No. 33) |
| Unit cell dimensions | |
| $a$ (Å) | 18.999(9) |
| $b$ (Å) | 8.389(4) |
| $c$ (Å) | 13.260(8) |
| $V$ (Å$^3$) | 2113(2) |
| $Z$ | 8 |
| $D_{calc}$ (Mg m$^{-3}$) | 1.861 |
| Wavelength (Å) | 0.71073 |
| $\mu$(Mo–K$_\alpha$) (cm$^{-1}$) | 21.5 |
| $\Theta$ range (°) | 2.1–22.5 |
| Reflections collected | 1390 |
| Reflections observed ($I>2\sigma(I)$) | 1273 |
| Data/parameters | 1390/137 |
| $R1$ [a], $wR2$ [b] ($I>2\sigma(I)$) | 0.052, 0.129 |
| $R1$ [a], $wR2$ [b] (all data) | 0.057, 0.135 |
| Goodness-of-fit on $F^2$ | 1.083 |

[a] $R_1 = \Sigma\|F_0|-|F_c\|/\Sigma|F_0|$.
[b] $wR_2 = \{\Sigma[w(F_0^2-F_c^2)^2]/\Sigma[w(F_0^2)^2]\}^{1/2}$.

[Pd($\eta^3$-1,1,2-$Me_3C_3H_2$)(HN–S–$^t$Bu)]$ClO_4$ (pale-yellow microcrystals);
[Pd($\eta^3$-1,1,2-$Me_3C_3H_2$)(HN–SPh)]$ClO_4$ (whitish microcrystals);
[Pd($\eta^3$-1,1,2-$Me_3C_3H_2$)(MeN–S–$^t$Bu)]$ClO_4$ (pale-yellow microcrystals);
[Pd($\eta^3$-1,1,2-$Me_3C_3H_2$)(MeN–SPh)]$ClO_4$ (whitish microcrystals);
[Pd($\eta^3$-1,1,2,3,3-$Me_5C_3$)(MeN–S–$^t$Bu)]$ClO_4$ (pale-yellow microcrystals); and
[Pd($\eta^3$-1,1,2,3,3-$Me_5C_3$)(MeN–SPh)]$ClO_4$ (pale-yellow microcrystals).

### 3.3. Solvents and reagents

Toluene and $CH_2Cl_2$ were distilled under inert atmosphere on Na/benzophenone and on $CaH_2$, respectively. All other chemicals were commercially available grade products.

#### 3.3.1. X-ray data collection and structure refinement of [PdCl(Me)(HN–SMe)]

Crystal data, summary of data collection and structure refinement details are collected in Table 4. Diffraction data were collected at r.t. on a single-crystal STOE four-circle diffractometer, using a yellow thin plane of dimension $0.30 \times 0.15 \times 0.05$ mm. Since the diffracting ability of the sample fell off rapidly with increasing Bragg angle, data collection was restricted to $2\Theta = 45°$. The structure amplitudes were obtained after the usual Lorentz and polarisation correction and data were corrected for absorption using the psi-scan method (maximum and minimum transmission factor of 0.92 and 0.48). The structure was solved by the heavy-atom method starting from three-dimensional Patterson map and refinement on $F^2$ was first done isotropically and subsequently with application of anisotropy only to the heavy and nitrogen atoms. The structure solution was based on the observed reflections, while the refinement was based on all reflections. The hydrogen atoms were placed in idealised positions and constrained to ride on the carbon atoms to which they are bonded. Their contributions were added to the structure factor calculations but their positions were not refined. The final difference map showed no unusual feature. Structure determination and refinement were performed with the SHELXTL NT program package [28].

### 3.4. IR, NMR and UV–vis measurements

The IR, $^1$H- and $^{13}C\{^1H\}$-NMR spectra were recorded on a Nicolet Magna™ 750 spectrophotometer and on a Bruker AC™ 200 or on a Varian 400™Unity, respectively. UV–vis spectra and kinetic measurements were performed on a Perkin–Elmer Lambda 40™ spectrophotometer equipped with a Perkin–Elmer PTP 6™ (Peltier Temperature Programmer) apparatus.

### 3.5. Kinetics measurements

The kinetics of allene insertions were studied by addition of known aliquots of allene solutions to solutions of the complex under study in $CH_2Cl_2$ ($[Pd]_0 \approx 10^{-4}$ mol dm$^{-3}$) in the thermostatted cell compartment of the spectrophotometer or by addition of known amounts of allene solutions to solutions of the complex under study in $CD_2Cl_2$ ($[Pd]_0 \approx 5 \times 10^{-2}$ mol dm$^{-3}$) into a 5 mm NMR tube. The reactions were followed by recording spectral changes in the wavelength range 250–350 nm and at a fixed suitable wavelength in the case of UV–vis technique or following the disappearance of Pd–C$H_3$ signal ($\delta \approx 1$ ppm) in the case of $^1$H-NMR studies. Kinetic measurements were performed either under pseudo-first or second-order conditions; mathematical and statistical data analysis was carried out on a personal computer equipped with a locally adapted version of Marquardt's algorithm [29] written in TURBOBASIC™.

## 4. Supplementary material

Final non-H atoms positional coordinates, bond distances and angles, anisotropic thermal parameters and atomic coordinates for hydrogens are available with the author on request.

## References


[1] L. Canovese, F. Visentin, G. Chessa, P. Uguagliati, G. Bandoli, Organometallics 19 (2000) 1461.

[2] (a) R.P. Hugues, J. Powel, J. Organomet. Chem. 20 (1969) 17;
(b) R.P. Hugues, J. Powel, J. Organomet. Chem. 60 (1973) 409;
(c) D. Medena, R. Van Helden, J. R. Neth. Chem. Soc. 90 (1971) 304;
(d) L. Besson, J. Goré, B. Cazes, Tetrahedron Lett. 36 (1995) 3853 and 3867;
(e) R. Grigg, M. Montheith, V Sridharan, C. Terrier, Tetrahedron 54 (1998) 3885;
(f) J.M. Zenner, R.C. Larock, J. Org. Chem. 64 (1999) 7312.

[3] (a) I. Shimuzu, J. Tsuji, J. Chem. Lett. (1984) 203;
(b) M. Ahmar, B. Cazes, J. Goré, Tetrahedron Lett. 25 (1984) 4505;
(c) M. Azhmar, B. Cazes, J.J. Barieux, J. Goré, Tetrahedron 43 (1987) 513;
(d) B. Cazes, Pure Appl. Chem. 62 (1990) 1867;
(e) P.W.N.M. van Leeuwen, G. van Koten, in: J.A. Moulijn, et al. (Eds.), Catalysis. An integrated approach to homogeneous, heterogeneous and industrial catalysis, Elsevier Science, Amsterdam, 1993 (and references therein);
(f) J.G.P. Delis, P.G. Aubel, K. Vrieze, P.W.N.M. van Leeuwen, Organometallics 16 (1997) 2948;
(g) A. Yamamoto, J. Chem. Soc. Dalton Trans. (1999) 1027;
(h) S. Mecking, Coord. Chem. Revs. 203 (2000) 325 (and refs therein);
(i) R. Zimmer, C.U. Dinesh, E. Nandanan, F.A. Khan, Chem. Rev. 100 (2000) 3067 (and Refs therein);
(l) T. Yagyu, M. Hamada, K. Osakada, T. Yamamoto, Organometallics 20 (2001) 1087.

[4] (a) P. Dierkes, P.W.N.M. van Leeuwen, J. Chem. Soc. Dalton Trans. (1999) 1519;
(b) P.G.C.M. Dekker, C.J. Elsevier, K. Vrieze, P.W.N.M. van Leeuwen, Organometallics 11 (1992) 1598;
(c) R. van Asselt, E.E.C.G. Gielens, R.E. Rülke, K. Vrieze, C.J. Elsevier, J. Am. Chem. Soc. 116 (1994) 977;
(d) H.A. Ankersmit, N. Veldman, A.L. Spek, K. Eriksen, K. Goubitz, K. Vrieze, G. van Koten, Inorg. Chim. Acta 252 (1996) 203;
(e) R.E. Rülke, J.G.P. Delis, A.M. Groot, C.J. Elsevier, P.W.N.M. van Leeuwen, K. Vrieze, K. Goubitz, H. Schenk, J. Organomet. Chem. 508 (1996) 109;
(f) J.H. Groen, C.J. Elsevier, K. Vrieze, W.J.J. Smeets, A.L. Spek, Organometallics 15 (1996) 3445;
(g) J.G.P. Delis, J.H. Groen, K. Vrieze, P.W.N.M. van Leeuwen, N. Veldman, A.L. Spek, Organometallics 16 (1997) 551;
(h) R.E. Rülke, V.E. Kaasjager, D. Kliphuis, C.J. Elsevier, P.W.N.M. van Leeuwen, K. Vrieze, K. Goubitz, Organometallics 15 (1996) 668;
(i) J.H. Groen, J.G.P. Delis, P.W.N.M. van Leeuwen, K. Vrieze, Organometallics 16 (1997) 68.

[5] L. Canovese, F. Visentin, G. Chessa, P. Uguagliati, A. Dolmella, J. Organomet. Chem. 601 (2000) 1.

[6] F.H. Allen, J.E. Davies, J.J. Galloy, O. Johnson, O. Kennard, C.F. Macrae, E.M. Mitchell, G.F. Mitchell, J.M. Smith, D.G. Watson, J. Chem. Inf. Comp. Sci. 31 (1999) 187.

[7] P.W.N.M. van Leeuwen, C. Roobeek, H. van der Heijden, J. Am. Chem. Soc. 116 (1994) 1217.

[8] (a) E. Abel, D.G. Evans, J.R. Koe, V. Sik, M.B. Hursthouse, P.A. Bates, J. Chem. Soc. Dalton Trans. (1989) 2315;
(b) E. Abel, J.C. Dormer, D. Ellis, K.G. Orrel, V. Sik, M.B. Hursthouse, M.H. Mazid, J. Chem. Soc. Dalton Trans. (1992) 1073.

[9] (a) J. Herrman, P.S. Pregosin, R. Salzmann, A. Albinati, Organometallics 14 (1995) 3311;
(b) M. Tschoerner, G. Trabesinger, A. Albinati, P.S. Pregosin, Organometallics 16 (1977) 3447;
(c) L. Canovese, F. Visentin, P. Uguagliati, G. Chessa, A. Pesce, J.Organomet. Chem. 566 (1998) 61.

[10] The collapse of the $CH_2S$ AB quartet was monitored in the cases of the complexes [PdCl(Me)(HN–SMe)], [PdCl(Me)(HN-S′Bu)] and [PdCl(Me)(MeN-S′Bu)] in the temperature range 183–298 K in $CDCl_3$. We could perform correct line shape simulations for the two exchanging systems with the DNMR5 program [11]. The uncertainty in the temperature determination was estimated at $\pm 3$ K whereas the errors on the kinetic constants were given by the program output (in any case $\Delta k/k$ was $\leq 0.1$). The kinetic constants at the given temperature were analysed by means of a weighted reparametrised Eyring equation [12]. In all cases the resulting activation entropy was found to be very small in absolute value, thereby confirming the intramolecular nature of the observed phenomenon. The $\Delta H^{\#}$ values (average $16 \pm 3$ Kcal $mol^{-1}$) are hardly influenced by the ancillary ligands and in line with those expected for sulphur inversion in palladium complexes [13].

[11] V.G. Stephenson, G. Binsch, DNMR5, Quantum Chemistry Program Exchange QCPE 365. Modified by C.B. LeMaster, C.L. LeMaster, N.S. True, Quantum Chemistry Program Exchange QCMP 059.

[12] P. Uguagliati, R.A. Michelin, U. Belluco, R. Ros, J. Organomet. Chem. 169 (1979) 115.

[13] L. Canovese, V. Lucchini, C. Santo, F. Visentin, A. Zambon, J. Organomet. Chem. 642 (2002) 58.

[14] The $pK_a$ values of 6-methylpyridine, pyridine and 6-chloropyridine are 6.00, 5.23 and 0.49, respectively. It would be reasonable for an analogous trend to be maintained in the pyridylthioether ligands. The basicity of the 6-chloropyridine derivatives would be at least five orders of magnitude smaller than that of the 6-methyl and 6-H analogs.

[15] G.P.C.M. Dekker, A. Buijs, C.J. Elsevier, K. Vrieze, P.W.N.M. van Leeuwen, W. Smeets, A.L. Spek, J.F. Wang, C. Stam, Organometallics 11 (1992) 1937.

[16] D.M. Adams, Metal Ligand and Related Vibrations, Arnold, London, 1967.

[17] R.E. Rülke, D. Kliphuis, C.J. Elsevier, J. Fraanje, K. Goubitz, P.W.N.M. van Leeuwen, K. Vrieze, J. Chem. Soc. Chem. Commun. (1994) 1817.

[18] H.A. Ankersmit, B.H. Løken, H. Kooijman, A.L. Spek, K. Vrieze, G. van Koten, Inorg. Chim. Acta 252 (1996) 141.

[19] (a) B.M. Trost, D.L. van Vranken, Chem. Rev. 96 (1996) 395;
(b) P.S. Pregosin, R. Salzmann, Coord. Chem. Rev. 155 (1996) 35.

[20] M.L. Tobe, J. Burgess, Inorganic Reactions Mechanisms, Addison Wesley, Longman, New York, 1999 (Chapter 3).

[21] F. Basolo, R.G. Pearson, Mechanism of Inorganic Reactions, Wiley, New York, 1967 (Chapter 5).

[22] E. Drent, P. Arnoldy, P.H.M. Budzelaar, J. Organomet. Chem. 455 (1993) 247.

[23] (a) V. De Felice, V.G. Albano, C. Castellani, M.E. Cucciolito, A. De Renzi, J. Organomet. Chem. 403 (1991) 269;
(b) F.P. Fanizzi, L. Maresca, G. Natile, M. Lanfranchi, A. Tiripicchio, G. Pacchioni, J. Chem. Soc. Chem. Commun. (1992) 333.

[24] J.H. Barnes, F.R. Hartley, C.E.L. Jones, Tetrahedron 38 (1982) 3277.

[25] K.C. Lee, D.Y. Chi, J. Org. Chem. 64 (1999) 8576.

[26] R.E. Rülke, J.M. Ernsting, A.L. Spek, C.J. Elsevier, P.W.N.M. van Leeuwen, K. Vrieze, Inorg. Chem. 32 (1993) 5769.

[27] J. Chatt, L.M. Vallarino, L.M. Venanzi, J. Chem. Soc. (1957) 3413.

[28] G.M. Sheldrick, SHELXTL NT ver. 5.10; Bruker Analytical X-ray Systems, Madison, WI, 1997.

[29] D.W. Marquardt, SIAM J. Appl. Math. 11 (1963) 431.